Implementation of GSA Based Optimal Lead-Lead Controller for Stabilization and Performance Enhancement of a DC Electromagnetic Levitation System

Mrinal Kanti Sarkar*, Subrata Banerjee*, Tapas Kumar Saha*, Sakti Prasad Ghoshal*

**National Institute of Technology, Durgapur, Department of Electrical Engineering, India-713209,*
(e-mail: itsmrinal2u@gmail.com, bansub2004@yahoo.com, tapassahanit@gmail.com, saktiprasad.ghoshal@ee.nitdgp.ac.in).

Abstract: In this paper, design, fabrication and testing of voltage controlled (singe loop) single actuator based attraction type levitation system has been reported. A cylindrical shaped hollow ferromagnetic object has been arranged to suspend under E-core electromagnet for some specific applications. The linearized model (transfer function) of voltage controlled electromagnetic levitation system (EMLS) is third order and unstable. Due to higher order structure tuning of controller parameters becomes more difficult for voltage controlled EMLS than current controlled second order EMLS. Usually controllers based on classical technique have been reported for the overall closed loop stabilization. These controllers have a restricted zone of operation and the tracking performance of the controller is found to deteriorate rapidly with increasing deviations from the nominal operating point for which the controller has been designed. As opposed to classical techniques, in this work, an optimization technique **is** presented that is aimed at a stabilizing controller of predefined order and structure which also yields good overall performance for a wide air-gap range of operation of the EMLS. The optimized parameters of cascaded two Lead controllers (Lead-Lead) for single actuator based voltage controlled EMLS are determined using a novel Gravitational Search Algorithm (GSA), implemented in dSPACE platform using MATLAB. Finally stability and performances are tested experimentally.

Keywords: Optimal Control, GSA, EMLS, Tracking Performance, Classical Control.

1. INTRODUCTION

The suspension of ferromagnetic object with the aid of magnetic force is termed as magnetic levitation or MAGLEV (Gotzein, 1984; Sinha, 1987; Boldea *et al.*, 1988 and Trica, 2009). Magnetic levitation system has received a lot of attention because it eliminates the frictional loss due to physical non-contact. They are becoming popular in two different kinds of application; high speed motion and precision engineering industry.

Depending on the principle of operation, there are two types of magnetic levitation systems. These are electro-dynamic levitation system (EDLS) and electromagnetic levitation system (EMLS). EMLS is based on the attractive force developed between the ferromagnetic object and the electromagnet. The DC attraction type levitation system is inherently unstable and nonlinear in nature. PD, Lead, Lag-Lead, PID and combination of these controllers have been mostly used (Banerjee *et al*., 2008; Jayawant, 1988) for obtaining the overall closed loop stability of current controlled EMLS. The resulting controllers have been tuned by extremely tedious and time consuming 'trial and error' process on the 's'-plane utilizing root-locus design concept. In case of voltage controlled EMLS controller the design becomes more difficult because the order of linearized models transfer function increases by one. Finding the suitable controller which will provide both stability and satisfactory performances becomes impossible by trial and error procedure. (Kaloust *et al*., 2004 and Queiroz *et al*., 1996) proposed recursive back stepping methods to control nonlinear magnetic levitation system. Three model-free control strategies which include a simple proportional-integral-differential (PID) control, a fuzzy-neural network (FNN) control and an adaptive control have been introduced by (Wai *et al*., 2005) for the positioning of a hybrid magnetic maglev system. (Wai *et al*., 2008) also introduced adaptive sliding-mode (SM) control and adaptive FNN control schemes for the levitation and propulsion control of a maglev transportation system. Some other possible solutions that have been reported in the literature are feedback linearizing control (Joo *et al*., 1997), Trumper *et al*., 1997) and H∞ control (Bittar *et al*., 1998) by considering the nonlinear model of the system.

Thus a proper optimization scheme for obtaining the optimized parameters of the proposed cascaded of two Lead (Lead-Lead) controller has to be developed so that the prototype EMLS may stably operate over a wide area maintaining good performance. For the tuning of the proposed Lead-Lead controller parameters to get optimized performance, Gravitational search Algorithm (GSA) has been utilized in the present work. Gravitational search algorithm (GSA) was introduced by (E. Rashedi *et al*., 2009). GSA is based on Newtonian law of gravity. This algorithm is simple to understand, easy to implement and gives the optimum convergence rate. In this work, a small prototype of single actuator based voltage controlled EMLS has been designed and developed. GSA is used to tune the proposed Lead-Lead controller parameters based on performance index objective/

fitness function minimization for obtaining the optimal performance of EMLS at nominal air gaps in the simulation. Finally, during actual experimentation, the prototype EMLS has been implemented in dSPACE platform using MATLAB. Simulation results have been validated through experimentation.

2. DESCRIPTION OF PROPOSED LEVITATION SYSTEM

A cylindrical shaped hollow ferromagnetic object is suspended under E-core electromagnet (Fig.1). When the electromagnet is excited, there is a force of attraction between the magnet and the ferromagnetic body. The typical attractive force versus air-gap characteristic with changing coil-current of the EMLS is given in Fig. 2. To have a stable levitation of the object at any operating point 'O', the attractive force developed between the magnet and the object should exactly balance the weight of the body. A vertical upward shift to decrease the air-gap produces an increase in the force of attraction; the net force is upwards, causing the body to attach itself to the magnet. Conversely a slight increase in the air gap by shifting down causes the body to fall away under the force of gravity. So to retain the suspended body in a stable position the field current of the electromagnet must be regulated quickly and accurately by sensing the coil current and object's position. Again for constant load application and with any change of operating point the force-airgap characteristic will get changed to accommodate the change in the coil-current as well as the attractive force developed between the magnet and the object (Fig.2).

So this levitation process is basically a problem of feedback control system and is represented in closed-loop form with different subsystems as shown in Fig.1. Here a position transducer senses the gap between the magnet pole-face and the ferromagnetic object and the output signal is fed back to a comparator. The output of comparator is applied to a controller which dynamically maintains the force balance ensuring closed loop stability of the system. The controller sends a command signal to the amplifier, which produces necessary currents in the actuator coils. The currents in the coils generate requisite magnetic forces.

One circular aluminium disc is mounted on the hollow steel cylinder symmetrically and is placed under DC electromagnet. This aluminium disc is used for extra damping during levitation.

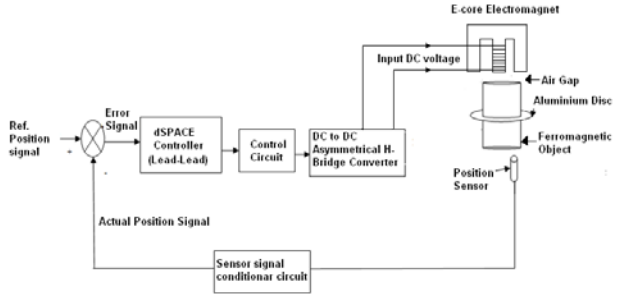

Fig. 1. Schematic block diagram of the proposed EMLS.

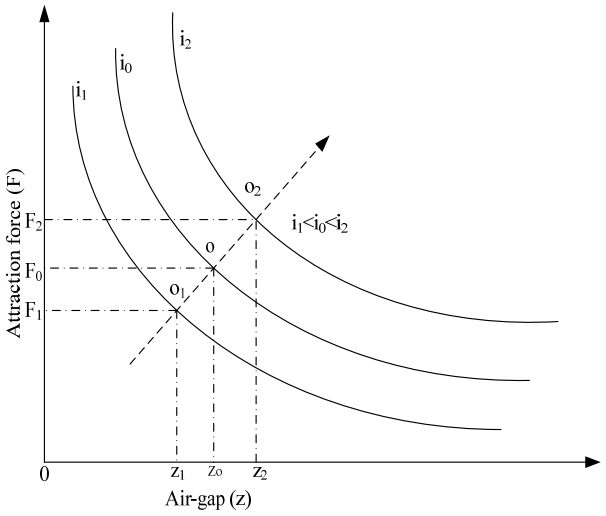

Fig. 2. Attraction force vs. air- gap characteristic between the magnet and the object.

During any oscillation or movement of the object eddy currents will be produced in the aluminium disc and these will produce a magnetic field which will oppose the main field produced by the electromagnet. In effect an extra damping force will be produced that will be helpful to reduce unwanted oscillations. Here the mass of the aluminium disc has been added to the cylinder while designing the controller parameters.

3. MODELING OF DC-ELECTROMAGNETIC LEVITATION SYSTEM

The DC attraction type levitation system is strongly nonlinear in nature due to the inherent nonlinearities of the electromagnetic circuit. Apart from magnetic saturation effects, the nonlinearities which have dominant influence on the stability of the suspended system are the magnetic force-distance -current characteristics, the effect of eddy currents on the moving object and the hysteresis in the magnetic core. The analysis and modeling of all these nonlinearities is really a complex matter and has not been considered in this work. To simplify the analysis and controller design a linearised model around an operating point has been used after the considering following assumptions:

• The overall magnetic circuit is assumed to be linear. Hysteresis and eddy current effects are neglected.

• Leakage flux is neglected and it is assumed that all magnetic flux generated by the electromagnet pass through the ferromagnetic object.

• The permeability of the magnetic material is assumed to be very high so that the complete magnetizing ampere-turns are utilized in the air gap.

• The resistance of the coil may change by a small value due to the increase in temperature after prolonged operation. But for simplicity it is assumed to be constant throughout the operation.

• Coil inductance is constant around the operating point, and any electromotive force owing to motion of the ferromagnetic object is neglected.

• The aluminium disc has been placed symmetrically on the object and it will not have any mechanical influence on the system. The eddy current effect produced on the disc during movement of object is not considered in modelling.

At any instant of time, the force of attraction between the electromagnet and the ferromagnetic object is given by

$$F(i,z) = -\frac{d}{dz}\left[\frac{1}{2}L(z)i^2\right] \tag{1}$$

To determine the inductance, the impedance of the coil is measured by AC volt–amp method at power frequency. The impedance is measured at different voltage levels and then the average value is taken for the calculation of the inductance. The same procedure is repeated for different air-gap positions by varying the object position through some mechanical arrangement. The experimental inductance profile of the levitated system with the change in the air-gap is shown in Fig. 3. The ferromagnetic object contributes to the inductance of the electromagnet coils. As the object approaches towards the magnet-coil inductance increases and as the object moves farther away from the electromagnet, the inductance decreases, reaching a minimal value when it is too far. This minimum value is, of course, the inductance of the magnet coil. From Fig. 3, it is clear that the inductance value (practical) around an operating point (in the medium-gap range) mostly varies inversely with respect to the object position and can be approximated as

$$L(z) = L_c + \frac{L_0 z_0}{z} \tag{2}$$

where L_c is the inductance of the coil in the absence of the object and L_0 is the additional inductance contributed by the ferromagnetic object. Now substituting (2) into the basic force equation (1), the following force *F(i,z)* is obtained.

$$F(i,z) = -\frac{i^2 dL(z)}{2dz} = c\left(\frac{i}{z}\right)^2 \tag{3}$$

where c is a constant, which can be determined experimentally and given as

$$c = \frac{L_0 z_0}{2} \tag{4}$$

So, at the equilibrium position (i_0, z_0) the normalized force equation is

$$F_0(i_0, z_0) = c\left[\frac{i_0}{z_0}\right]^2 = mg \tag{5}$$

The dynamics of the ferromagnetic cylindrical object is given by the following equation (6).

$$m\ddot{z} = -F(i,z) + mg = -c\left[\frac{i}{z}\right]^2 + mg \tag{6}$$

The system dynamic equations are thus nonlinear and hence difficult to analyze. So the equations are linearised around a suitable operating point (i_0, z_0) and the linearised model may be found as described below. If the mass of the object is displaced by an amount Δz from the steady-state position, then the corresponding changes in current and force are, respectively, Δi and ΔF. Here, the coil-current i may be assumed as a composition of two parts: a steady-state component (i_0) which generates the vertical attractive force at an equilibrium point (i_0, z_0), and a much smaller component Δi which provides the attraction force for balancing any variation around the equilibrium point (i_0, z_0).The small perturbation linear equations (discounting second order effects) of the system are:

$$m\ddot{z} = -c\left[\frac{i_0 + \Delta i}{z_0 + \Delta z}\right]^2 + mg$$

$$= -K_a \Delta i + K_z \Delta z \tag{7}$$

Thus, $K_a = 2c\left(\frac{i_0}{z_0^2}\right)$ and $K_z = 2c\left(\frac{i_0^2}{z_0^3}\right)$ (8)

Two force constants (K_a and K_z) are determined from the inductance and current profiles (Fig.3 and Fig.4).

The current-gap characteristic of the levitated system is determined as follows: A variable DC supply is used to apply a slowly increasing voltage to the magnet coil. The coil current is read using an ammeter. When the magnet current is small the upward electromagnetic attraction force is smaller than the downward pull offered due to gravity and hence the object does not move. For a particular operating gap the exact current at which the object just lifts is noted. This measurement procedure is carried on for different air-gaps between the magnet and the object.

The plot of pick-up current (which is assumed to be close to levitation current) versus air-gap for the EMLS is shown in Fig. 4.

Taking Laplace transforms on both the sides of (7) and after rearranging, the transfer function of the current controlled plant is

$$G_{pi}(s) = \frac{\Delta Z(s)}{\Delta I(s)} = -\frac{\left(\frac{K_a}{m}\right)}{\left(s + \sqrt{\frac{K_z}{m}}\right)\left(s - \sqrt{\frac{K_z}{m}}\right)} \tag{9}$$

It is assumed that when the system is properly designed, the suspended object will remain close to its equilibrium

position, i.e., $z=z_0$, the total inductance L(z) becomes constant L for the particular gap length, z_0 (operating point) and hence independent of position z. Thus from (2), the expression of total inductance can be expressed as follows:

$$L = L_c + L_0 \tag{10}$$

The instantaneous voltage equation across the magnet winding is

$$v = Ri + \frac{d}{dt}[Li] \tag{11}$$

If there is a change in the voltage Δv for which there is a change in the current Δi, the voltage equation (11) can be written as

$$\Delta v = R\Delta i + L\frac{d\Delta i}{dt} \tag{12}$$

where v_0 is the steady state voltage and i_0 is the steady state current. Thus we can write

$$v_0 = i_0 R \tag{13}$$

Taking Laplace transform of (12),

$$\frac{\Delta I(s)}{\Delta V(s)} = \frac{1}{R + sL} \tag{14}$$

So the transfer function of the plant in case of controlled voltage source can be written as

$$G_p(s) = \frac{\Delta Z(s)}{\Delta V(s)} = -\frac{1}{(R+sL)} \frac{\left(\frac{K_a}{m}\right)}{\left(s+\sqrt{\frac{K_z}{m}}\right)\left(s-\sqrt{\frac{K_z}{m}}\right)} \tag{15}$$

The negative sign in the expression indicates the decrease of the object position with the incremental change of coil current or force.

From Table-1 and using (2), (8) and (15), the computed expression of the transfer function of the voltage controlled EMLS is given below

$$G_p(s) = -\frac{9.7}{(0.0693s + 2.3499)(s+38.15)(s-38.15)} \tag{16}$$

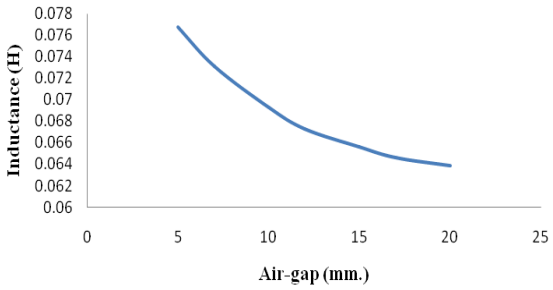

Fig. 3. Inductance vs. air gap.

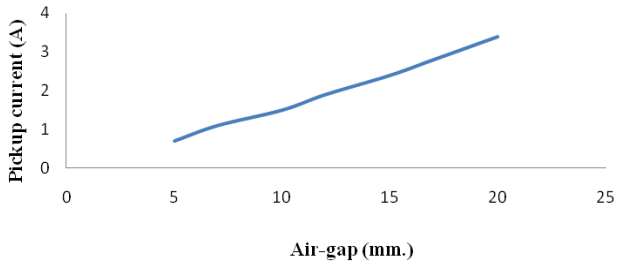

Fig. 4. Pick-up current vs. air gap.

Table 1. Parameters for the single actuator based EMLS.

Parameters	Values
Mass of the object	0.119kg
Resistance of the coil	2.349Ω
Inductance of the coil(L_c)	0.0616H
Operating air gap (z_0)	0.01m
Inductance at 0.01m air gap (L)	0.0693H
Incremental inductance (L_0)	0.0077H
Pick up current at 0.01m air gap (i_0)	1.5A
Position sensor gain	1000V/m

4. CONTROLLER DESIGN

In the linearized model the transfer function of voltage controlled EMLS is of third order and unstable as shown in (16). In majority cases the unstable levitation system has been stabilized in closed loop using single Lead controller (Dragomir *et al*., 2001 and Dragomir *et al*., 2003). But one such controller could not provide both stability and satisfactory performance for such unstable system. In this paper, two Lead controllers are used in cascaded form (Lead-Lead) for better stability and performance. The transfer function of resultant controller is given below

$$G_c(s) = \frac{K(s+\hat{Z}_1)(s+\hat{Z}_2)}{(s+P_1)(s+P_2)} \tag{17}$$

Here, K is the constant gain; $\hat{Z}_1$, $\hat{Z}_2$ are zeros and P_1, P_2 are poles of the two Lead controllers. The parameters (K, $\hat{Z}_1$, $\hat{Z}_2$, P_1 and P_2) have to be optimized for obtaining the optimal performance of the proposed levitated system. The detail of the proposed optimal control is given below.

4.1 Objective function for GSA

To obtain the optimum performance of a system under varying conditions of operation, a performance index or fitness function or objective function is required, which is a function of variable system parameters. Minimum value of this performance index or objective function/ fitness function then corresponds to the optimum set of parameter values. To evaluate fitness of each particle or agent fitness function is evaluated. The selection of fitness functions is the most crucial step in applying GSA. A number of such performance

indices or fitness functions are used in practice; these are Integral of the Square Error (ISE), Integral of the Absolute magnitude of Error (IAE), Integral of Time multiplied by Absolute Error (ITAE) and Integral of Time Square Error (ITSE). ITAE is the most sensitive among other three performance indices. In this case, for ITAE steady state error is less but percentage overshoot is very high. To make trade off between steady state error and percentage overshoot, the fitness function is considered as the combination of ITAE and percentage overshoot. The expression of the fitness function is given below

$$fit(t) = \int_{o}^{T} t\left|e(t)dt\right| + \frac{\hat{M}_p}{\lambda} \tag{18}$$

The limits for the equation $t = 0$ to t_s, where t_s is the settling time of the system or multiple of settling time. $\hat{M}_p$ and $e(t)$ are percentage overshoot and error, respectively. λ is weighing factor. In this study, λ has been chosen as 0.35. The statements justifying λ=0.35 are given in the section 7 (Simulation results).

4.2 Gravitational Search Algorithm

This optimization algorithm is based on law of gravity (Rashedi *et al*., 2009; Chaterjee *et al*., 2011). In GSA, agents are considered as objects and their performance is measured by their masses. All these objects attract each other by the gravity force, and this force causes a global movement of all objects towards the objects with heavier masses. Hence, masses cooperate using a direct form of communication through gravitational force. The heavy masses (which correspond to good solutions) move more slowly than lighter ones. This guarantees the exploitation step of the algorithm. Three kinds of masses are defined in theoretical physics:

(a) Active gravitational mass (M_a) is a measure of the strength of the gravitational field due to a particular object. (b) Passive gravitational mass (M_p) is a measure of the strength of an object's interaction with the gravitational field. (c) Inertial mass (M_q) is a measure of an object's resistance to changing its state of motion when a force is applied. An object with large inertial mass changes its motion more slowly, and an object with small inertial mass changes it rapidly.

In GSA, each mass (agent) has four specifications viz. position, inertial mass, active gravitational mass, and passive gravitational mass. The position of the mass corresponds to the solution of the problem, and its gravitational and inertial masses are determined using a fitness function. In other words, each mass presents a solution, the algorithm is navigated by properly adjusting the gravitational, and inertial masses. By lapse of time, it is expected that masses be attracted by the heaviest mass. This mass will present an optimum solution in the search space.

The GSA could be considered as an isolated system of masses. It is like a small artificial world of masses obeying the Newtonian laws of gravitation and motion. More precisely, masses obey the following two laws.

i. Law of gravity: Each particle attracts every other particle and the gravitational force between two particles is directly proportional to the product of their masses and inversely proportional to the square of the distance (D) between them. (Rashedi *et al*., 2009; Chaterjee *et al*., 2011) used D instead of D^2 because D offered better results than D^2 in all their experimental cases with benchmark functions. Using single exponent instead of double exponent for D causes the departure of the present GSA from exact Newtonian Law of gravitation.

ii. Law of motion: The current velocity of any mass is equal to the sum of the fraction of its previous velocity and the variation in the velocity. Variation in the velocity or acceleration of any mass is equal to the force acted on the system divided by the mass of inertia.

The position of the q^{th} agent among n_p total number of agent vectors (population) is defined as

$$X_q = (X_q^1, X_q^2, X_q^3, ..., X_q^d, .., X_q^n), \text{ for } q=1,2,3\ldots\ldots n_p. \tag{19}$$

where X_q^d presents the position of q^{th} agent vector in the d^{th} dimension and n is total number of dimensions.

In our study each agent vector of the population n_p denotes five parameters /dimension (X_q^1 =constant gain (K), $X_q^2 = 1^{st}$ zero($\hat{Z}_1$), $X_q^3 = 2^{nd}$ zero($\hat{Z}_2$), $X_q^4 = 1^{st}$ pole (P_1) and $X_q^5 = 2^{nd}$ pole(P_2)) of Lead-Lead controller.

At a particular time "t", the force acting on mass "q" from mass "j" is given in (20).

$$F_{qj}^d(t) = G(t)\frac{M_{pq}(t)\times M_{aj}(t)}{D_{qj}(t)+\varepsilon}(X_j^d(t) - X_q^d(t)) \tag{20}$$

Here, M_{aj} is the active mass and M_{pq} is the passive mass related to the agents q and j, respectively. $D_{qj}(t)$ is the Euclidean distance between two agents q and j.

$$D_{qj}(t) = \left\| X_q(t), X_j(t) \right\|_2 \tag{21}$$

The gravitational constant G at iteration t

$$G(t) = G_0 e^{-\alpha\left(\frac{t}{t_{\max}}\right)} \tag{22}$$

here G_0 and α are constant and $t_{\max}$ is the maximum number of iteration.

To introduce stochastic characteristic of the net force $F_q^d(t)$ acting on the agent "*q*", the following expression is given in (23), using (20).

$$F_q^d(t) = \sum_{j=1, j\neq q}^{n_p} rand_j F_{qj}^d(t) \tag{23}$$

where the $rand_j$ is random number in the interval of [0,1]. The technique is used to perform a good compromise between exploration and exploitation is to decrease the number of agents with lapse of iteration number in (23). Therefore, only a set of agents with higher masses apply their forces to others but it may decrease the exploration power and increase the exploitation capability. To control exploration and exploitation, only *Kbest* agents will attract each other. *Kbest* is the function of iteration cycle number. *Kbest* is computed in such a manner that it decreases linearly with time and at last iteration the value of Kbest becomes 2% of the initial number of agents. Now, the modified force equation becomes

$$F_q^d(t) = \sum_{j\in Kbest, j\neq q} rand_j F_{qj}^d(t) \tag{24}$$

According to the law of motion, the acceleration of q^{th} agent at d^{th} direction,

$$a_q^d(t) = \frac{F_q^d(t)}{M_{qq}(t)} \tag{25}$$

where $M_{qq}(t)$ is the inertial mass of the q^{th} agent.

The velocity and position updating formulae are given below

$$v_q^d(t+1) = rand_q \times v_q^d(t) + a_q^d(t) \tag{26}$$

$$X_q^d(t+1) = X_q^d(t) + v_q^d(t+1) \tag{27}$$

where the $rand_q$ is random number in the interval of [0,1]. The gravitational and inertial masses are calculated using (29) and (30).

$$M_{aq} = M_{pq} = M_{qq} = M_q \quad \text{where} \quad q=1,2,3\ldots\ldots\ldots n_p. \tag{28}$$

$$\hat{m}_q(t) = \frac{fit_q(t) - worst(t)}{best(t) - worst(t)} \tag{29}$$

$$M_q = \frac{\hat{m}_q(t)}{\sum_{j=1}^{n_p} \hat{m}_q(t)} \tag{30}$$

where $fit_q(t)$ represent the fitness value of the agent *q* at time *t*, and, *worst(t)* and *best(t)* are defined as follows:

$$best(t) = \min_{j\in\{1,\ldots,n_p\}} fit_j(t) \tag{31}$$

$$worst(t) = \max_{j\in\{1,\ldots,n_p\}} fit_j(t) \tag{32}$$

The flow chart of GSA has been given in Fig.5.

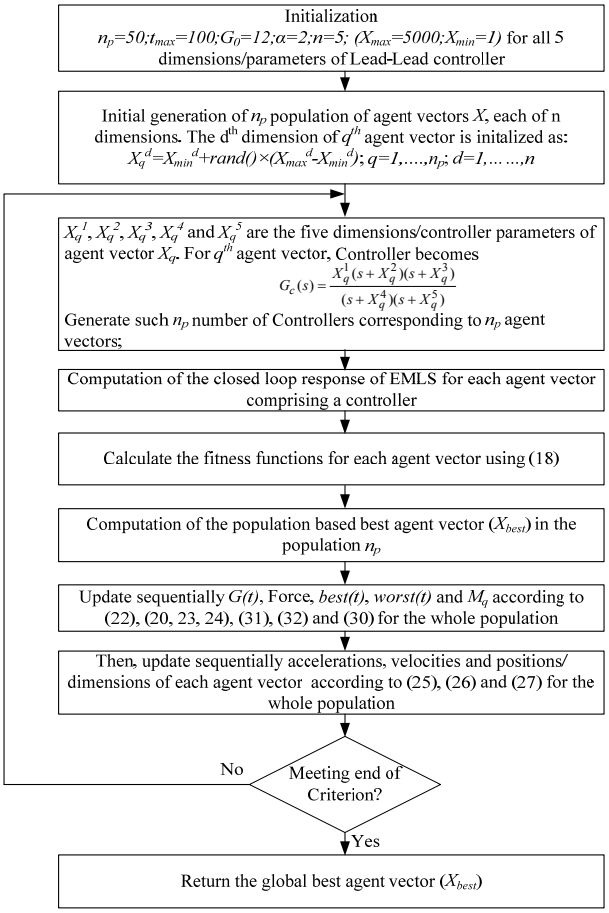

Fig. 5. Flowchart of GSA.

5. DESCRIPTION OF EXPERIMENTAL SET-UP

The parameters of levitated system are shown in Table-1. The layout of dSPACE based control system of the proposed EMLS is shown in Fig.6. An inductive type position sensor is used to measure the relative air gap between the magnet pole face and the object. The output of the position sensor is

filtered by a low pass filter and compared with the reference signal which generates an error signal. Here the coil-current is excited by controlled voltage source and only position control loop is used. So the requirement of costly current sensor is dispensed with in this system. The air-gap between the pole face of magnet and cylindrical object has been sensed with Contrinex make inductive type position sensor. The output signal of the position sensor is found to be noisy due to high frequency electromagnetic interference from the switched mode chopper circuit. The position signal needs to be made noise-free before being fed to the dSPACE using ADC channel-5. There are several stages of filtering used in the overall control circuit. A simple R-C type low pass filter is connected after the position sensor output. After placing the values of R (100K) and C (0.02 F), the transfer function of the filter becomes

$$G_{f1}(s) = \frac{500}{(s+500)} \tag{33}$$

The cut-off frequency of this low pass filter is around 80 Hz and it has a unity DC gain. The filtered position signal is compared to the reference gap signal in a low pass (first order) type differential amplifier having a DC gain of unity and having a transfer function as given by (34).

$$G_{f2}(s) = \frac{1000}{(s+1000)} \tag{34}$$

The differential amplifier helps to remove common mode noise from the signal. The differential amplifier has low-pass characteristics due to the capacitors in the forward gain of the amplifier. Thus any high frequency noise due to MOSFET switching etc. is attenuated. The output of this differential circuit is clamped to ± 4.7 Volts before being fed to dSPACE controller.The gap-error is then processed through the Lead-Lead controller using Simulink block in DS1104, the output of which generates PWM control signal. This PWM signal is passed through the control circuit which provides isolation and amplification before applying to the gate of IGBT. The dSPACE system is described as a real-time interface (RTI) and works as a link between the computer modeling framework in Simulink and the hardware. The dSPACE hardware used in this work is the DS1104 R&D Controller Board with CP1104 Connector Panel. The DS1104 has a 64-bit floating-point MPC8240 processor working at 250 MHz with on-chip peripherals. The peripherals include one 16-bit analog to digital converter (ADC) with four muxed channels, four 12-bit ADCs, digital I/O ports, serial interface and more. The ADC channels are used to read the analog signals from the position and current sensors.

The DAC channels are used to read digital signals from dSPACE. The hardware also includes a Slave DSP subsystem composed by a Texas Instruments TMS320F240 DSP working at 20 MHz. The slave subsystem is responsible for the PWM outputs.

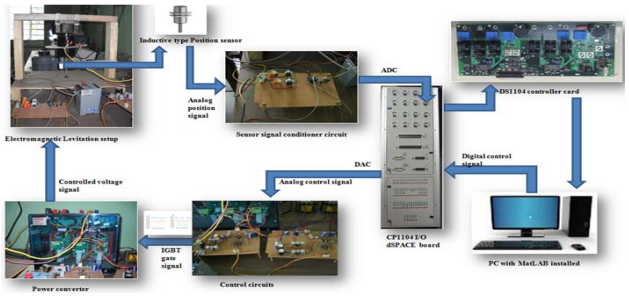

Fig. 6. Layout of dSPACE based control of Electromagnetic Levitation System.

6. DESCRIPTION OF POWER CIRCUIT

The magnet used in this prototype is generally large and has large time constant (L/R ratio). The effective air-gap between the magnet pole face and the cylindrical shape ferromagnetic object is small. The electro-magnetic force is generally large and unless there is fast control of the magnetic coil current by controlling the coil voltage the levitating object will either be falling on the position sensor or will be hitting the magnet pole face of the E-core electromagnet. The coil current needs to rise and fall in accordance with the control signal generated by the position controller. The expected variation in the demand current (small signal component) of the magnet, over its nominal DC value, is expected to be band limited to around 10 Hz but it is better to have a current tracking capability in the range up to 100 Hz. The electrical time constant of the magnet being large, the amplifier needs to apply considerably large instantaneous voltages to the magnet coil (larger in comparison to the DC voltage required to maintain just the nominal current) for allowing quick control of the coil current. In this present work asymmetrical H-bridge converter is used (Fig. 7).The asymmetrical bridge circuit requires only half the number of switches and diodes than the full bridge circuit and is capable of applying bi-directional load voltage similar to the full bridge circuit. Within each high frequency cycle as the switches are ON, positive voltage across the coil causes the coil current to rise and during OFF duration, coil current falls due to the application of negative voltage. During the fall of current through the diodes, part of the magnet energy is fed back to the supply and is not required to dissipate through any external resistance and thus the circuit is quite energy efficient. Because of its high energy-efficiency this asymmetric converter is ideal for high power applications. Ohmic isolation is required between the gate drive signals of the two controlled switches and this calls for proper isolation and amplification stage for driving each of the two switches.

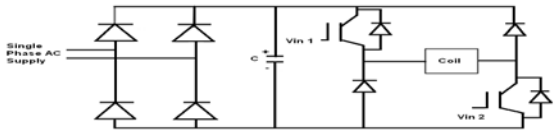

Fig. 7. Block diagram of Power Converter circuit.

When gate pulse coming to drive IGBTs (ON period), the energy flow takes place from source to sink (coil). During OFF period polarity of the coil gets changed and the diodes get forward-bias. The duty cycle is calculated using (35)

$$\delta = \frac{1}{2}\left(\frac{V_0}{V_{in}} + 1\right) \tag{35}$$

Here duty cycle is represent by δ and V_0 and V_{in} are output and input voltage respectively. The switching frequency of the power converter is around 5kHz.

7. SIMULATION RESULTS

For simulation, the five dimentational (n=5) search space has been initialized randomly. G_0=12, α=2, n_p =50 and t_{max}=100.

The justification for the choice of λ=0.35 is as given below:

Magnetic levitation system is always prone to instability. So, if the percentage overshoot becomes more, the object may hit the magnet. On the other hand, if the steady state error becomes more, the position error of the object is high, which is also not desirable. λ=0.1 causes high steady state error but low percentage overshoot. Whereas λ=1 causes low steady state error but high percentage overshoot. λ=0.35 yields moderate values of both percentage overshoot and steady state error. So, λ=0.35 is the best compromising value, as shown in Fig. 8 from the simulation study.

The simulations are done by using the linearized model of the EMLS. It is found in experimental results that the controller parameters corresponding to λ=0.35 result in much less overshoot but more steady state error as compared to those of the simulation results. The other λ values considered in the simulation test cause very much inferior results in the experimental results. This has occurred due to inherent nonlinearities present in actual practice and not taken into account in the simulation. So, finally, λ=0.35 is considered as the best value for the experimental study.

The weightage factor is chosen as 1/λ. If λ is a proper fraction, then the minimization of percentage overshoot is more stressed, though the time weightage associated with the steady state error will also be highly effective for minimization of the steady state error.

In Fig. 9, the convergence curve of the fitness function corresponding to λ=0.35 lies in the middle of two curves corresponding to λ values 0.1 and 1. Both the steady state error and percentage overshoot are moderate and not high for λ=0.35.

Though the percentage overshoot has been reduced due to high (>1) weightage factor 1/λ (λ=*0.35*) the time weightage associated with the steady state error has caused the first factor of the fitness function dominating over the second factor of reduction of percentage overshoot of the same function; the overall fitness function value has increased and the corresponding fitness curve has shifted up. The low steady state error corresponding to λ=0.1 has caused the fitness curve to be lowered down with reference to that corresponding to λ=0.35. Fig. 9 justifies the above statements.

The transfer function obtained for the GSA based optimal Lead-Lead controller is given below

$$G_c(s) = \frac{4065.05(s+44)(s+43.062)}{(s+1554.4)(s+1000)} \tag{36}$$

The root-locus plot of the overall closed-loop system utilising a Lead- Lead compensator is shown in Fig. 10.

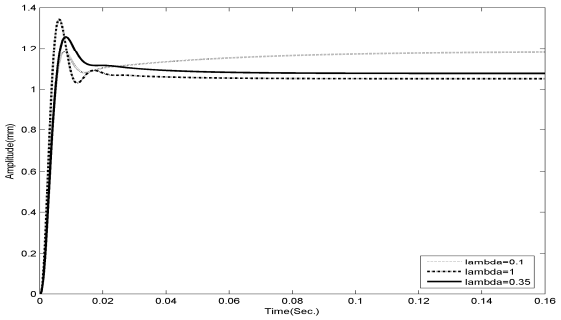

Fig. 8. Step response of closed loop system for different values of λ.

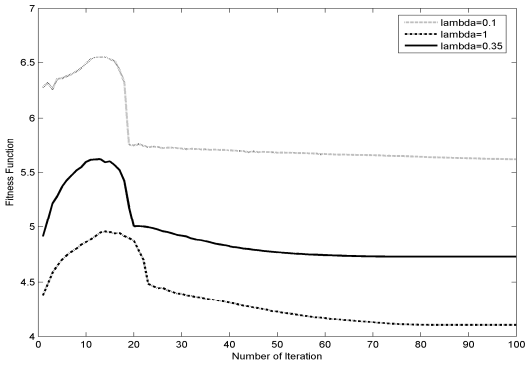

Fig. 9. Convergence curves of fitness function for different λ values.

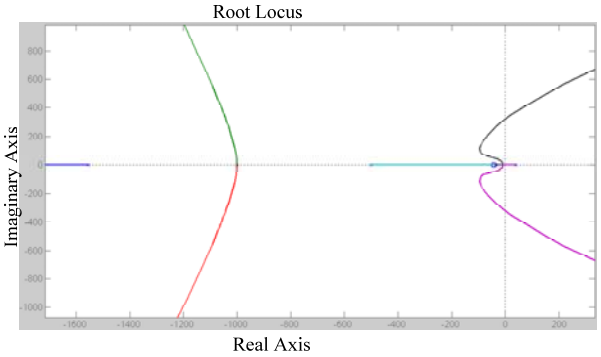

Fig. 10. Root-locus plot of the overall closed-loop system utilising a GSA-Lead-Lead compensator.

8. EXPERIMENTAL RESULTS

The effectiveness of the proposed control scheme is investigated via implementation of the experimental set-up. Fig. 11 shows the experimental set-up. Fig. 12 shows the gate pulse (CH-1), coil voltage (CH-2), position signal (CH-3) and coil current (CH-4) during the stable levitation of the object. Same gate pulse is fed to 2-IGBTs gates of the asymmetrical H-bridge converter. When the gate pulses are high, switches (2-IGBTs) are turned on, the full positive supply voltage appears across the coil and the coil current increases. When the gate pulse is negative, switches are turned off, the two diodes conduct, negative supply voltage appears across the coil and the coil current decreases. Fig. 13 shows current (CH-4) and position signals (CH-3) during stable levitation of the cylindrical object. It appears that position signal is a little bit oscillatory, but the ripple may be neglected as compared to the DC magnitude. When the object tries to move upwards, the output of position sensor increases, but due to the decrease in air-gap between the pole face of electromagnet and the object coil-current reduces and vice-versa.

To study the dynamic performance of any system generally different tests are conducted. One way to verify the operation of the physical system is to create step changes to the desired position in order to observe the system's transient behaviour. Fig. 14 shows the position responses of the levitated object at nominal operating gap position (0.001m) utilizing optimized parameters of Lead-Lead controller.

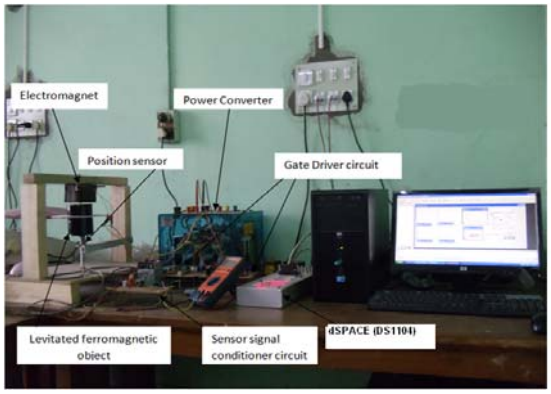

Fig. 11. Complete hardware set-up for the levitation system.

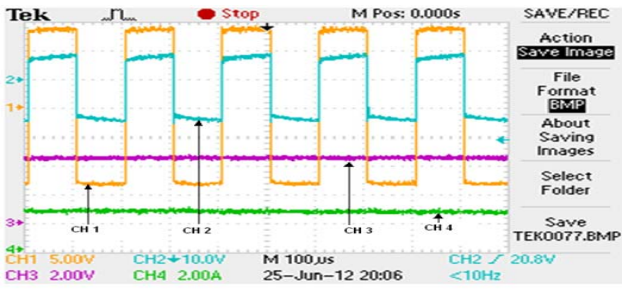

Fig. 12. Gate pulse (CH-1), Coil voltage (CH-2), Position signal (CH-3) and Coil current (CH-4) during stable levitation.

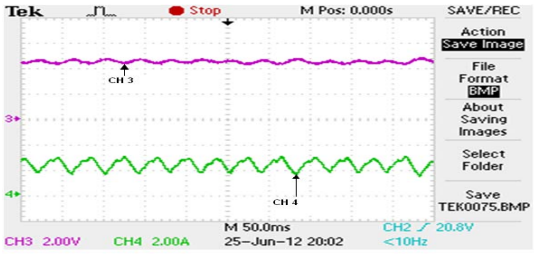

Fig. 13. Position signal (CH-3) and coil current signal (CH-4).

Here, the controller designed for a fixed air-gap is fed with a steady gap command superimposed with a small repetitive step voltage. It is seen that with the use of optimized Lead-Lead controller (Fig. 14) the closed loop position response becomes stable, faster and produces satisfactory transient performance with zero overshoot (0%). The dynamic current signal is also captured which shows satisfactory transient and steady state responses. But steady-state error (8%) is present in the position response because Lead-Lead controller cannot eliminate the steady-state error. Fig. 15 shows how the position and current signals track the reference triangular input during stable movement of the object. It is clear that the output position signal exactly matches with the reference triangular waveform with a difference in the DC bias.

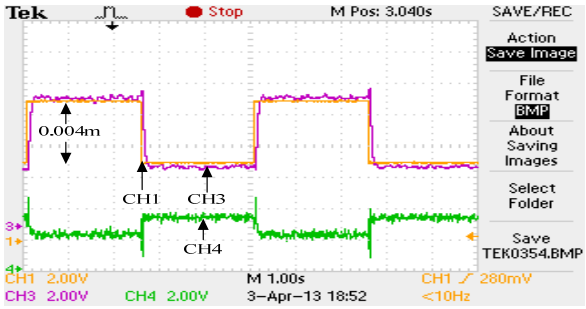

Fig. 14. Dynamic position (CH3) and current response (CH4) due to the square wave step input (CH1).

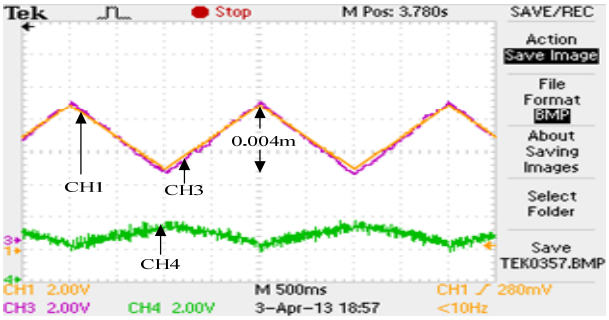

Fig. 15. Dynamic position (CH3) and current response (CH4) due to the triangular wave input (CH1).

9. CONCLUSION

In this work, design, development and testing of voltage controlled single actuator based EMLS have been performed.

The parameters of proposed Lead-Lead controller are optimized using Gravitational Search Algorithm and the designed controller is implemented in DSP environment. Simulation results are validated by experimentation successfully. From experimental results it is clear that the proposed optimized GSA based Lead-Lead controller stabilizes the unstable maglev system and provides satisfactory performance at the desired operating air-gap. Here the magnet coil-current is excited by a controlled voltage source, so only single position control loop is used. Though the design of the position controller is simpler in current controlled system, implementation of one more loop will incur extra cost which is not desirable. Other different advanced controllers may be implemented with the existing set-up and that will be a future extension of this work.

ACKNOWLEDGEMENT

The authors wish to acknowledge DST, Govt. of India for sponsoring the Project No.SR/S3/EECE/0008/2010 entitled "Development of DC Electromagnetic Levitation Systems – Suitable for Specific Industrial Applications".

REFERENCES

Banerjee, S., Sunil Kumar, T.K., Pal, J., and Prasad, D. (2008). Controller Design for Large-Gap Control of Electromagnetically Levitated System by using an Optimization Technique, *IEEE Transactions on Control Systems Technology*, Vol. 16, Issue 3, pp.408-415.

Bittar, A., and Sales, R.M. (1998). H2 and H∞ control for maglev vehicles, *IEEE Control System Magazine*, Vol. 18, no. 4, pp. 18-25.

Boldea, Ion., Trica, A., Papusoiij, G. and Nasar, S. A. (1988). Field Tests on a MAGLEV with Passive Guideway Linear Inductor Motor Transportation System*, IEEE Trans. on Vehicular Technology*, Vol. 37, No. 4, pp.213-219.

Chaterjee, A., Ghoshal, S. P., and Mukherjee, V. (2011). Gravitational Search Algorithm with wavelet mutation for the solution of economic load dispatch problems, *International Journal of Bio-Inspired Computation*, Vol. 4, No.1, pp. 33-46.

Dragomir T. L., Silea I. (2001). Control Problems related to a Balancing Machine with Magnetic Bearings, *Proceedings of the 9th IFAC/IFORS/IMACS/IFIP-Large Scale Systems 2001 Symposium*, Bucharest, July, pg. 120-125.

Dragomir, T.L., Silea, I. (2003). Control system for the magnetic bearings of a balancing machine, *Journal of Electric Engineering*, 3, 1, pp.21-26, ISSN 1582-4594.

Gotzein, E. (1984). Magnetic wheel as an autonomous entity modular levitation and guidance systems for magnetic way, *VDI-Verlag, Dusseldorf*, Munich, ISBN 3-18-146808-8.

Jayawant, B.V. (1988). Review lecture on electromagnetic suspension and levitation techniques, *Proc. Ro. Soc. London*, A416, pp.245-320.

Joo, S., and Seo, J. H. (1997). Design and analysis of the nonlinear feedback linearizing control for an electromagnetic suspension system, *IEEE Trans. on Control Systems Technology*, Vol. 5, No. 1, pp.593-598.

Kaloust, J., Ham, C., Siehling, J., Jongekryg, E., and Han, Q. (2004). Nonlinear robust control design for levitation and propulsion of a maglev system, *Proc. Inst. Elect. Eng.—Control Theory Appl.,* Vol. 151, No. 4, pp. 460–464

Queiroz, M. S., and Dawson, D. M. (1996). Nonlinear control of active magnetic bearings: A back stepping approach, *IEEE Trans. Control Systems Technology*, Vol. 4, No. 5, pp. 545–552.

Rashedi, E., Nezamabadi-pour, H., and Saryazdi, S. (2009). GSA: A Gravitational Search Algorithm, *Information Sciences*, 179, Pp. 2232-2248.

Sinha, P. K. (1987). Electromagnetic Suspension, *Dynamics and Control, London: Peter Peregrinus Ltd.*

Trica, A. R. (2009). Sustentation Electromagnetic Systems, *Politehnica Publishing Hous*, ISBN-9736259072, 9789736259074.

Trumper, D., Olson, S. M., and Subrahmanyan, P. K. (1997). Linearizing control of magnetic suspension system, *IEEE Trans. on Control Systems Technology*, Vol. 5, No. 4, pp. 427-438.

Wai, R. J., and Lee, J. D. (2005). Performance comparisons of model-free control strategies for hybrid magnetic levitation system, Proc. *Inst. Elect.Eng.—Elect. Power Appl.*, Vol. 152, No. 6, pp. 1556–1564.

Wai, R. J., and Lee, J. D. (2008). Adaptive fuzzy-neural-network control for maglev transportation system*, IEEE Trans. Neural Netw*., Vol. 19, No. 1, pp. 54–70.